13

Testing the Standard Model

Precision Measurements of the Z and W; Search for the Higgs.

The ψ and Υ resonances were startling and largely unanticipated. By contrast, it was apparent far in advance that the Z would be spectacular in e^+e^-annihilation. Indeed, within the Standard Model nearly every aspect of the Z could be predicted to the extent that $\sin^2\theta_W$ was known. Despite this, the study of the Z in e^+e^-annihilation was a singular achievement in particle physics.

After initial planning as early as 1976, CERN began construction of the Large Electron Positron collider in 1983. Because ultrarelativistic electrons lose energy rapidly through synchrotron radiation, whose intensity varies as E^4/ρ, where ρ is the radius of curvature, LEP was designed with a large circumference, 26.67 km. The first collisions occurred on August 13, 1989.

In a daring move, SLAC aimed to reach the Z before LEP by colliding electron and positron beams generated with its linear accelerator. At the Stanford Linear Collider each bunch would be lost after colliding with the opposing bunch. While the Mark II detector, which had seen service at PEP, was refurbished, four new detectors – ALEPH, DELPHI, L3, and OPAL – were built at CERN.

SLC indeed got to the Z first (Ref. 13.1), but with a disappointing luminosity. In July 1989, Mark II reported for the Z a mass of 91.11 ± 0.23 GeV and a width of $1.61\,^{+0.60}_{-0.43}$ GeV, based on 106 events.

These results were soon surpassed by measurements at Fermilab. The original accelerator at Fermilab began operation in 1972 with an energy of 200 GeV. At the time of the discovery of the Υ in 1977, it was operating at 400 GeV. Fermilab pioneered the use of superconducting magnets, which increased the operating field to 4 T, allowing the beam energy to be doubled to 800 GeV. Following the lead of the SPS at CERN, Fermilab also constructed a ring in which antiprotons could be accumulated. The Tevatron Collider brought together protons and antiprotons inside the main ring. Through this series of improvements, the operating c.m. energy of the machine increased from about $\sqrt{s} = 20$ GeV to $\sqrt{s} = 1.6$ TeV, from which it was subsequently raised to 1.8 TeV.

The first detector at the Tevatron Collider was CDF, the Collider Detector Facility. A descendant of UA1 and UA2, CDF featured cylindrical geometry, tracking with a drift

Downloaded from https://www.cambridge.org/core. UNIVERSIDAD AUTONOMA METROPOLITANA, on 10 Nov 2026 at 11:33:25, subject to the Cambridge Core terms of use, available at https://www.cambridge.org/core/terms. https://doi.org/10.1017/9780511609923.015

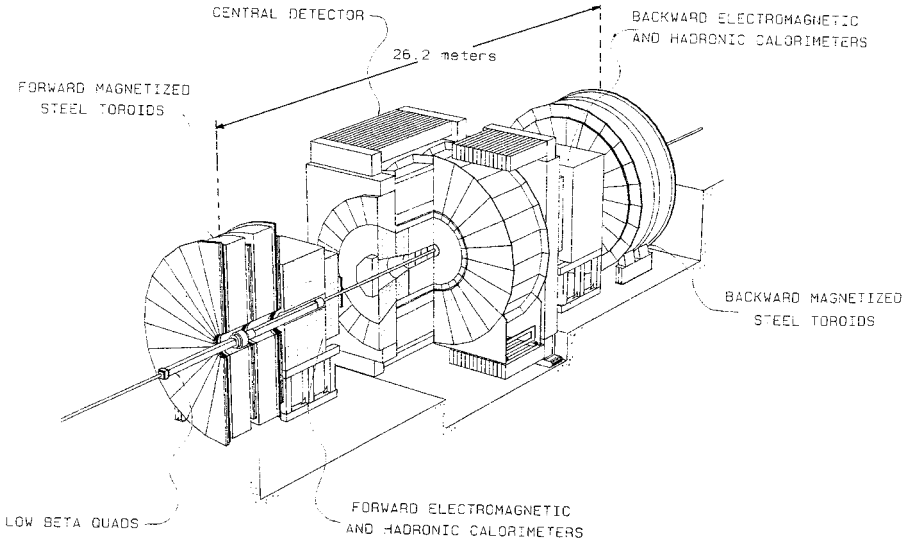


Figure 13.1. The CDF detector circa 1988. From the inside out, the major sections are the inner detector, the electromagnetic and hadronic calorimeters, and finally the magnetized steel toroids for muon identification and measurement. [Courtesy Fermilab and CDF Collaboration.]

chamber inside an axial magnetic field of 1.4 T, and both electromagnetic and hadronic calorimetry outside the magnet. The final layer provided for muon detection and measurement. During the 1988/89 run, a total of 4 pb^{-1} was accumulated.

A second detector at the Tevatron Collider, D0, was completed in 1992. It complemented CDF by optimizing calorimetry at the cost of tracking. In particular, it had no magnetic field in its tracking region. D0's advantage lay in measuring jets at high transverse momentum and in detecting missing transverse momentum, a sign of neutrinos or other non-interacting particles. The energies of electrons and muons could be measured using electromagnetic calorimetry for the former and magnetized absorbers in the outermost layers for the latter.

CDF, pursuing the hadron collider path set by UA-1 and UA-2, found a Z mass of $90.9 \pm 0.3 \pm 0.2$ GeV and a width $3.8 \pm 0.8 \pm 1.0$ GeV (Ref. 13.2) from 188 events. Back at SLAC, Mark II announced new results in October 1989, based on 480 events: $m_Z = 91.14 \pm 0.12$ GeV, $\Gamma_Z = 2.42^{+0.45}_{-0.35}$ GeV.

The high precision measurement of initial interest was the full line shape of the Z because it would reveal the total number of light neutrinos that couple to the Z. While the apparent number was simply three – ν_e, ν_μ, ν_τ – additional generations would appear if their neutrinos were light even if their charged leptons and quarks were too heavy to be produced.

The shape of the Z resonance is determined primarily by the Breit–Wigner form discussed in Chapters 5 and 9. A relativistic version for e^+e^- annihilation through the Z to

Downloaded from https://www.cambridge.org/core. UNIVERSIDAD AUTONOMA METROPOLITANA, on 10 Nov 2026 at 11:33:25, subject to the Cambridge Core terms of use, available at https://www.cambridge.org/core/terms. https://doi.org/10.1017/9780511609923.015

produce the final state f at cm energy $\sqrt{s}$ is

$$\sigma_f(s) = \frac{12\pi}{m_Z^2}\frac{\Gamma_e\Gamma_f}{\Gamma^2}\frac{s\Gamma^2}{(s-m_Z^2)^2 + s^2\Gamma^2/m_Z^2}. \tag{13.1}$$

Here Γ represents the full width of the Z including its decays to neutrinos, while Γ_f represents the partial width into some final state f and in particular Γ_e is the partial width into e^+e^-. Because the light electrons and positrons can emit photons before annihilating, there is an important radiative correction. This reduces the height at the peak and makes the shape asymmetric. The cross section is higher above the peak than below it because the higher energy electrons and positrons can lose energy and move closer to the resonance.

From the fit to the line shape, the full width Γ could be determined. The peak cross section (with radiative corrections removed) is

$$\sigma_{peak} = \frac{12\pi}{m_Z^2}\text{BR}(\ell)\ \text{BR(had)} \tag{13.2}$$

where BR(had) is the branching ratio for Z into hadrons and BR(ℓ) is the branching ratio for the Z into one of the three charged leptons, assuming the three to be equal. The relative frequency of the charged lepton and hadronic final states, $R_\ell = \text{BR(had)}/\text{BR}(\ell)$, could be measured as well. From Γ_Z, σ_{peak}, and R_ℓ, the partial widths Γ_ℓ and $\Gamma_{hadrons}$ could be deduced. If the remainder is assumed to be due to N_ν species of neutrinos, we can write

$$\Gamma = \Gamma_{hadrons} + 3\Gamma_\ell + N_\nu\Gamma_\nu \tag{13.3}$$

where Γ_ν is the partial width of the Z into a single neutrino species. If the Standard Model prediction is used for this quantity, then the number of neutrino species can be derived. The original Mark II data gave $N_\nu = 3.8 \pm 1.4$. With 480 events, the result was $N_\nu = 2.8 \pm 0.6$, with $N_\nu = 3.9$ excluded at 95% CL.

In November 1989, the LEP experiments reported their first results, each with a few thousand events (Refs. 13.3, **13.4**, 13.5, 13.6). The masses clustered near 91.1 GeV with uncertainties less than 100 MeV. The widths were all near 2.5 GeV, with uncertainties typically 150 MeV. The number of neutrino generations was found to be near three, with each experiment having an uncertainty of about 0.5. Together, the evidence was overwhelmingly for precisely three neutrino generations.

LEP studied the Z from 1989 to 1995 and tested the Standard Model in exquisite detail. The LEP detectors followed the conventional scheme of a generally cylindrical design, with charged-particle tracking close to the interaction point, followed by electromagnetic calorimetry, hadronic calorimetry, and finally by muon identification and measurement. Still, each detector had its own character. ALEPH and DELPHI both used large time projection chambers for tracking, with axial magnetic fields of 1.5 T and 1.2 T respectively. See Figure 13.2. The OPAL and L3 detectors used magnetic fields of 0.5 T. The magnet for L3 was outside the rest of the detector, providing an enormous volume over which muons could be tracked to give excellent measurements of their momenta.

Downloaded from https://www.cambridge.org/core. UNIVERSIDAD AUTONOMA METROPOLITANA, on 10 Nov 2026 at 11:33:25, subject to the Cambridge Core terms of use, available at https://www.cambridge.org/core/terms. https://doi.org/10.1017/9780511609923.015

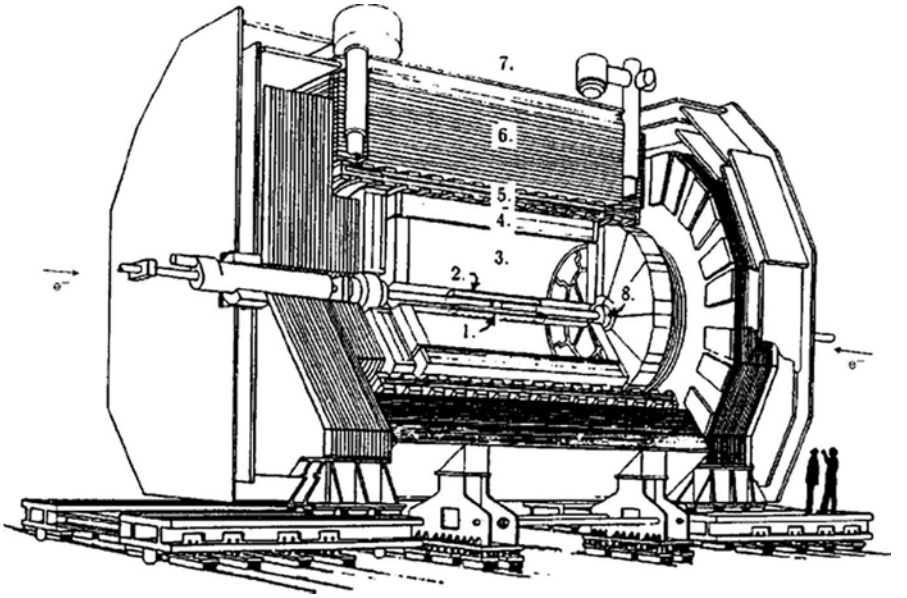


Figure 13.2. Cut-away view of the ALEPH detector at LEP showing (1) the silicon vertex detector, (2) inner trigger chamber, (3) time projection chamber, (4) electromagnetic calorimeter, (5) superconducting coil, (6) hadron calorimeter, (7) muon chambers, (8) luminosity monitors. Figure taken from M. Martinez *et al*., *Rev. Mod. Phys.* **71**, 575 (1999).

The tremendous number of events accumulated by the LEP detectors did not guarantee high precision results. Critical to this goal were accurate measurements of the luminosity and the beam energy. Cross sections could be measured only as well as luminosities and the Z mass only as well as the beam energy. Each detector monitored the luminosity by measuring Bhabha scattering, whose cross section is well known and whose rate is so large that statistics were basically unlimited. Ultimately, with very careful measurements of the luminosity monitor geometries, uncertainties were reduced below one part in a thousand.

The beam energy at LEP was measured with extreme accuracy by using the technique of resonant depolarization. This technique, developed at Novosibirsk where it was used to measure the mass of the J/ψ to high precision, resulted in a measurement of the beam energy to approximately 1 MeV once effects from the Earth's tides and the Geneva train system were fully understood.

The thousands of events grew to 16 million, shared between the four detectors. The most precise results were ultimately obtained by combining the data from ALEPH, DELPHI, L3 and OPAL, with the results $m_Z = 91.1876 \pm 0.0021$ GeV and $\Gamma_Z = 2.4952 \pm 0.0023$ GeV. The high precision measurement of the mass of the Z is especially important because it, together with $\alpha = 1/137.03599911 \pm 0.00000046$, and $G_F = 1.16637 \pm 0.00001 \times 10^{-5}$ GeV^{-2} can be taken as the three inputs that define the fundamental constants of the Standard Model. The peak cross section was found to be 41.540 ± 0.037 nb and the ratio of the hadronic to leptonic width was given by $R_\ell = 20.767 \pm 0.025$.

Downloaded from https://www.cambridge.org/core. UNIVERSIDAD AUTONOMA METROPOLITANA, on 10 Nov 2026 at 11:33:25, subject to the Cambridge Core terms of use, available at https://www.cambridge.org/core/terms. https://doi.org/10.1017/9780511609923.015

The Standard Model, described in Chapter 12 is a theory rather than a model in that it gives complete predictions, not just approximations. Every prediction can be expressed in terms of the three fundamental physical quantities, α, G_F, and m_Z. Other parameters of the Standard Model, like the quark and lepton masses can enter, as well. In practice, all the quark masses are small compared to the scale m_Z except for the mass of the top quark, to be discussed in Chapter 14. The mass of the Higgs boson, M_H, plays a role, too, but the dependence in radiative corrections turns out to be on $\ln M_H^2$ rather than on M_H^2 directly. Two kinds of radiative corrections turn out to be dominant: those involving m_t and the shift from using α evaluated as the static constant, $\alpha = 1/137.036...$, and α evaluated at the short distance given by the Compton wavelength of the Z. Because we are interested in processes at the energy scale m_Z, the expressions are simplest when written in terms of $\alpha(m_Z) \approx 1/129$.

The LEP program was to measure branching ratios, asymmetries, and polarizations, which could be compared to Standard Model results, looking for possible discrepancies that could signal new particles or forces.

The Standard Model makes very explicit predictions for the branching ratios of the Z. Using the relations given in Chapter 12, we find that for a decay to a left-handed fermion (and a right-handed antifermion),

$$\Gamma(Z \to f_L \overline{f}_R) = \frac{\sqrt{2} G_F m_Z^3}{6\pi} (T_3 - Q \sin^2 \theta_W)^2 \tag{13.4}$$

where Q is the charge of the fermion, T_3 is its third component of weak isospin ($1/2$ for u, c, $-1/2$ for d, s, and b) and θ_W is the weak mixing angle. If the fermion is a quark rather than a lepton, we must multiply by a color factor of three. For right-handed fermions (and left-handed antifermions), we have similarly,

$$\Gamma(Z \to f_R \overline{f}_L) = \frac{\sqrt{2} G_F m_Z^3}{6\pi} (Q \sin^2 \theta_W)^2. \tag{13.5}$$

There is a correction from QCD for the width to quark pairs, which in lowest order is a factor $1 + \frac{\alpha_s}{\pi} \approx 1.03$.

The angular dependence of the production of the various fermion pairs is governed by the simple expressions analogous to those given in Chapter 8, which reflect angular momentum conservation. Because the Z has only vector and axial vector couplings to fermions a left-handed electron can annihilate only a right-handed positron. If the electron's direction is the z-axis, the pair annihilates into a Z with $J_z = -1$. If the final fermion f is left-handed, then the antifermion is right-handed and angular momentum conservation prevents the fermion from coming out in the negative z direction. Thus we find

$$\frac{d\sigma}{d\Omega}(e_L^- e_R^+ \to Z \to f_L \overline{f}_R) \quad \propto \quad (1 + \cos\theta)^2 \tag{13.6}$$

$$\frac{d\sigma}{d\Omega}(e_L^- e_R^+ \to Z \to f_R \overline{f}_L) \quad \propto \quad (1 - \cos\theta)^2 \tag{13.7}$$

$$\frac{d\sigma}{d\Omega}(e_R^- e_L^+ \to Z \to f_L \overline{f}_R) \quad \propto \quad (1 - \cos\theta)^2 \tag{13.8}$$

Downloaded from https://www.cambridge.org/core. UNIVERSIDAD AUTONOMA METROPOLITANA, on 10 Nov 2026 at 11:33:25, subject to the Cambridge Core terms of use, available at https://www.cambridge.org/core/terms. https://doi.org/10.1017/9780511609923.015

$$\frac{d\sigma}{d\Omega}(e_R^- e_L^+ \to Z \to f_R \overline{f}_L) \quad \propto \quad (1+\cos\theta)^2 \tag{13.9}$$

Since the cross sections are proportional to $\Gamma_e \Gamma_f$ we have for unpolarized scattering

$$\frac{d\sigma}{d\Omega} \quad (e^- e^+ \to Z \to f\overline{f}) \\ \propto [\Gamma_{e_L} + \Gamma_{e_R}][\Gamma_{f_L} + \Gamma_{f_R}](1+\cos^2\theta) + 2[\Gamma_{e_L} - \Gamma_{e_R}][\Gamma_{f_L} - \Gamma_{f_R}]\cos\theta. \tag{13.10}$$

An asymmetry can be formed by comparing the number of events F in which the fermion f goes forward, that is, into the hemisphere in the electron's direction to the number B in which f goes into the backward hemisphere. We find

$$A_{FB}^f \equiv \frac{F-B}{F+B} = \frac{3}{4}\frac{[\Gamma_{e_L} - \Gamma_{e_R}]}{[\Gamma_{e_L} + \Gamma_{e_R}]}\frac{[\Gamma_{f_L} - \Gamma_{f_R}]}{[\Gamma_{f_L} + \Gamma_{f_R}]} \equiv \frac{3}{4}\mathcal{A}_e\mathcal{A}_f \tag{13.11}$$

where $\mathcal{A}_f = (\Gamma_{f_L} - \Gamma_{f_R})/(\Gamma_{f_L} + \Gamma_{f_R})$. The measurement of the forward–backward asymmetry in $e^+e^- \to Z \to \mu^+\mu^-$, for example, provides a clean measurement of $\sin^2\theta_W$ since we have

$$\mathcal{A}_\ell = \frac{1 - 4\sin^2\theta_W}{(1-2\sin^2\theta_W)^2 + 4\sin^4\theta_W}. \tag{13.12}$$

The combined LEP result was $A_{FB}^\ell = 0.0169 \pm 0.0013$.

The SLC's luminosity improved over the years, though it never rivaled that at LEP. Still SLC did have a capability that made it competitive for this class of measurements: beam polarization. Using the same technique that was used in the measurement of the left–right asymmetry in deep inelastic scattering of electrons off protons discussed in Chapter 12, left-handed and right-handed electrons were injected into the SLAC linac. It was not necessary to polarize the positrons since the coupling only allows annihilation of pairs with parallel spins.

An asymmetry can be formed for left-handed and right-handed electrons producing any final state, f. That asymmetry is simply equal to $\mathcal{A}_e$. If the degree of polarization of the beams is P, then $\mathcal{A}_e$ is simply given by $1/P$ times the observed asymmetry. Ultimately, an electron polarization of about 80% was achieved. The careful measurement of the polarization by scattering a polarized beam from the polarized electron beam was essential to the measurement. The result reported in 1997 by the SLD Collaboration (Ref. 13.7) was $\mathcal{A}_e = 0.151 \pm 0.011$, equivalent to $A_{FB}^\ell = 0.0171 \pm 0.0025$. The final analysis of the full data set gave an improved result, $\mathcal{A}_e = 0.1516 \pm 0.0021$, equivalent to $A_{FB}^\ell = 0.0171 \pm 0.0005$, consistent with the LEP result, but more precise.

Downloaded from https://www.cambridge.org/core. UNIVERSIDAD AUTONOMA METROPOLITANA, on 10 Nov 2026 at 11:33:25, subject to the Cambridge Core terms of use, available at https://www.cambridge.org/core/terms. https://doi.org/10.1017/9780511609923.015

With the measurement of the Z mass pinned down, the third fundamental parameter of the Standard Model, the measurement of the W mass became a critical test. The basic prediction for the W mass is

$$m_W^2 = \frac{\pi\alpha}{\sqrt{2}G_F \sin^2\theta_W} \tag{13.13}$$

where $\sin^2\theta_W$ itself depends on m_W:

$$\sin^2\theta_W = 1 - \frac{m_W^2}{m_Z^2}. \tag{13.14}$$

This is modified by radiative corrections. However, the dominant correction is simply to replace the usual fine structure constant $\alpha(0)$ by $\alpha(m_Z^2)$. Additional corrections depend on m_t^2 and $\ln(m_H/m_Z)$. See Problem 13.5. Thus a precision measurement of the W mass could predict the mass of the top quark, with only a weak dependence on the unknown mass of the Higgs boson.

While e^+e^- annihilation provided an unbeatable method for studying the Z, LEP was not suited for studying the W. The original measurements of the W mass by UA-1 and UA-2 had uncertainties of several GeV. In 1990, CDF reported on 1722 events combining results from the $W \to e\nu$ and $W \to \mu\nu$ channels. CDF found $m_W = 79.91 \pm 0.39$ GeV. By 1992, UA-2 had reduced the error by accumulating more than 2000 events of the decay $W \to e\nu$. For the ratio m_W/m_Z they found $0.8813 \pm 0.0036 \pm 0.0019$. The ratio could be determined more precisely than either value separately because some of the uncertainties were common to the two measurements. At the time, the mass of the Z had already been measured to ± 20 MeV at LEP, giving a combined result of $m_W = 80.35 \pm 0.33(\text{stat.}) \pm 0.017(\text{syst.})$ GeV.

In Run I at the Fermilab Tevatron Collider, from 1992 to 1995, CDF and D0 both accumulated large numbers of W's and Z's. The errors for each experiment were reduced to near 100 MeV, with a combined result of 80.450 ± 0.063 GeV, reported in 1999.

An entirely new approach to measuring the W mass became possible once the energy at LEP was increased above the WW threshold in June, 1996. The W pair cross section rises gradually rather than abruptly because the substantial width of the W makes it possible to produce one real and one virtual W. While one can measure the W mass through careful determination of the threshold rise, in fact the method found more effective at LEP-II was to reconstruct the mass from final states in $W \to q\overline{q}$, $W \to q\overline{q}$ and $W \to q\overline{q}$, $W \to \ell\nu$ events.

In 1997, more than 50 pb^{-1} of data were accumulated near $\sqrt{s} = 180$ GeV. The mass of the W could be determined with a statistical uncertainty of about 130 MeV by each experiment. Combining the experiments gave $80.38 \pm 0.07 \pm 0.03 \pm 0.02$ GeV, with the uncertainties arising from the experiment itself, from theoretical issues, and from the LEP beam energy. Further measurements were made as the c.m. energy was increased up to 206 GeV. The combined LEP result was $m_W = 80.376 \pm 0.033$ GeV. An upgraded CDF detector, running at the Tevatron Collider's Run II, remeasured the W with greatly increased

Downloaded from https://www.cambridge.org/core. UNIVERSIDAD AUTONOMA METROPOLITANA, on 10 Nov 2026 at 11:33:25, subject to the Cambridge Core terms of use, available at https://www.cambridge.org/core/terms. https://doi.org/10.1017/9780511609923.015

statistics and found a result in 2007 completely compatible with CERN's, $m_W = 80.413 \pm 0.048$ GeV.

Even before the discovery of the top quark in 1995, the W mass measurements were accurate enough to predict m_t to be around 180 GeV, assuming the Higgs mass was in the range of 100–1000 GeV.

The Higgs boson is the least constrained part of the Standard Model. Indeed, there is no a priori limit on its mass. If the mass is sufficiently large, more than say 1.5 TeV, the width of the Higgs boson becomes comparable to its mass and it is hard to justify calling it a particle at all. On the other hand, there is no reason to suppose that there is just a single Higgs boson. Indeed some models, like supersymmetry, require that there be more than one neutral Higgs boson. Because the Higgs boson couples feebly to light particles (that is why they are light!), it is best sought in conjunction with heavy particles. LEP II offered an ideal approach: $e^+e^- \to ZH$. The electron–positron pair annihilate into a virtual Z, which then decays to a real Z and the Higgs boson. In this way, a Higgs boson could be found up to very near the kinematic limit, $m_H = \sqrt{s} - m_Z$.

The Higgs boson couples to fermion pairs according to their masses, making $H \to b\overline{b}$ and $H \to \tau^+\tau^-$ the best targets. The accompanying Z can be detected in any of its decay channels. One vexing background comes from the ZZ final state, when one Z decays to $b\overline{b}$. With data taken at a center-of-mass energy of 189 GeV, three of the LEP experiments were able to set lower limits of about 95 GeV on a Standard Model Higgs boson, while the limit from ALEPH, the remaining experiment, was about 90 GeV.

Still there was more to be wrung out of LEP. Between 1995 and 1999 one after another upgrade was carried out to raise the energy higher and higher, opening each time a new window in which the Higgs boson might appear. The enormous effort this entailed was justified because detailed fits, which depended on $\ln m_H^2$, of the electroweak data from the Z pointed to a low value of the Higgs mass, around 100 GeV. The center-of-mass energy leapt to 204 GeV, then in a series of small steps to 209.2 GeV. No sign of a Higgs boson was seen until the data at 206 GeV were analyzed.

In the fall of 2000, ALEPH reported events above the background expected, consistent with a Higgs boson with a mass of 115 GeV. Some confirmation came from L3, but none from DELPHI or OPAL. Combining the data from all events in November 2000, the signal had a 2.9 σ significance. Luciano Maiani, the Director General of CERN faced a dilemma. Should he continue to raise the energy of LEP2 and accept a delay in CERN's next big project, the Large Hadron Collider, which was to use the LEP tunnel? The decision was made to terminate LEP2. Further analysis of the data in the summer of 2001 showed that the effect was somewhat smaller, 2.2 σ, but whether there is a 115-GeV Higgs boson will be settled by a hadron collider.

Exercises

13.1 Use the final LEP values for the width of the Z, σ_{peak}, and R_ℓ to determine N_ν. For Γ_ν / Γ_ℓ use the Standard Model value of 1.99.

Downloaded from https://www.cambridge.org/core. UNIVERSIDAD AUTONOMA METROPOLITANA, on 10 Nov 2026 at 11:33:25, subject to the Cambridge Core terms of use, available at https://www.cambridge.org/core/terms. https://doi.org/10.1017/9780511609923.015

13.2 Determine the expression for the left–right forward–backward asymmetry for the production of a fermion-antifermion pair at the Z when the initial electron polarization is P. How well can $\mathcal{A}_\mu$ be measured with N events of $e^+e^- \to \mu^+\mu^-$? Assume $\mathcal{A}_e$ is known from measuring the total cross section for left- and right-polarized electrons. Take $P = 0.75$. How much is the measurement of $\mathcal{A}_\mu$ improved by using polarized beams? Compare your estimate with SLC Collaboration, K.Abe *et al.*, *Phys. Rev. Lett.* **86**, 1162 (2001).

13.3 If a τ at rest decays, the angular distribution of the pion is $dN/d\cos\theta \propto 1 + \cos\theta$, where θ is the angle between the pion's direction and the spin of the τ and the mass of the pion is neglected. Show that this is consistent with the V-A nature of weak interactions. If a high energy τ decays to $\pi\nu$, what is the expected distribution of its visible energy, i.e. the pion's energy, if the τ is left-handed? Consider $Z \to \tau^+\tau^-$ and let $x = E_\pi/E_\tau$ be the fraction of τ's energy that is given to the π. Find the joint distribution in θ, the polar angle relative to the e^- direction and x, in terms of $\mathcal{A}_e$ and $\mathcal{A}_\tau$. See, ALEPH Collaboration, A. Heister *et al.*, *Eur. Phys. J.* **C20**, 401 (2001).

13.4 The stored LEP electron beam develops a polarization perpendicular to the plane of the ring. As described in Problem 12.4, the electron's spin makes $\nu_0 = \gamma a_e = (E_{beam}/m_e)a_e$ cycles around its polarization for each circuit of the ring, where $a_e \approx \alpha/2\pi$ is the anomalous magnetic moment of the electron in Bohr magnetons. Determine the value of ν_0 when LEP ran at the Z using the more precise value $a_e = 0.0115965$. At a single spot, the electron's spin will seem to advance only by $[\nu_0]$, the non-integer part of ν_0. If a radial magnetic field is applied with a frequency $[\nu_0]$ times the frequency of the electron's revolution around the ring, electron spins will flip, destroying or reversing the polarization. At LEP, the frequency of the depolarizing resonance was measured to 2 Hz. What uncertainty in the mass of the Z would this cause? See L. Arnaudon *et al.*, *Zeit. f. Phys.* **C66**, 45 (1995).

13.5 The W mass can be predicted from the Z mass using the formula

$$m_W^2 = \frac{1}{2}\left[1 + \sqrt{1 - \frac{4\pi\alpha(1+\Delta r)}{\sqrt{2}m_Z^2 G)F}}\right] m_Z^2$$

where Δr incorporates the radiative corrections, including the shift of α from its static value to the value at the scale m_Z. The radiative corrections depend on the value of m_t and m_H. An adequate representation [A. Ferroglila *et al.*, *Phys. Rev.* **D65**, 113002 (2002)] is

$$\begin{aligned} m_W(\text{GeV}) = 80.387 &- 0.572\ln(m_H/100\text{ GeV}) - 0.0090\,[\ln(m_H/100\text{ GeV})]^2 \\ &+ 0.540\,[(m_t/174.3\text{ GeV})^2 - 1]. \end{aligned}$$

Compare the current measurements of m_t and m_W. What does this indicate about the mass of the Higgs boson? Compare with the direct information from LEP II.

13.6 A value of $\sin^2\theta_W$ can be inferred from measurements of the forward–backward asymmetry at LEP. Within the Standard Model, it can be predicted in terms of the

Downloaded from https://www.cambridge.org/core. UNIVERSIDAD AUTONOMA METROPOLITANA, on 10 Nov 2026 at 11:33:25, subject to the Cambridge Core terms of use, available at https://www.cambridge.org/core/terms. https://doi.org/10.1017/9780511609923.015

three basic parameters, α, G_F, and m_Z if m_t and m_H are known. The latter two occur through radiative corrections. An adequate representation is

$$\begin{aligned}\sin^2\theta_{eff}^{lept} = &0.2314 + 4.9\times10^{-4}\ln(m_H/100\text{ GeV})\\ &+ 3.41\times10^{-5}\,[\ln(m_H/100\text{ GeV})]^2\\ &- 2.7\times10^{3}\,[(m_t/174.3\text{ GeV})^2 - 1].\end{aligned}$$

The results from LEP for the forward–backward asymmetry for leptonic final states gave $\sin^2\theta_{eff}^{lept} = 0.23113(21)$ while for hadronic final states the result was $\sin^2\theta_{eff}^{lept} = 0.23220(29)$. What do these results suggest about the mass of the Higgs? Compare with the results of Exercise 13.5.

Further Reading

ALEPH, DELPHI, L3, OPAL, and SLD Collaborations, LEP Electroweak Working Group, SLD Electroweak and Heavy Flavor Working Groups, "Precision Electroweak Measurements at the Z Resonance," *Phys. Rep.* **427**, 257 (2006).

References

13.1 G. A. Abrams *et al.*, "Initial Measurements of Z-boson Resonance Parameters in e^+e^- Annihilation." *Phys. Rev. Lett.*, **63**, 724 (1989).
13.2 F. Abe *et al.*, "Measurement of the Mass and Width of the Z^0 Boson at the Fermilab Tevatron." *Phys. Rev. Lett.*, **63**, 720 (1989).
13.3 L3, "A Determination of the Properties of the Neutral Intermediate Vector Boson Z0." *Phys. Lett.*, **B 231**, 509 (1989).
13.4 ALEPH , "The Number of Light Neutrino Species." *Phys. Lett.*, **B 231**, 519 (1989).
13.5 OPAL, "Measurement of the Z^0 Mass and Width with the OPAL Detector at LEP." *Phys. Lett.*, **B 231**, 530 (1989).
13.6 DELPHI, "Measurement of the Mass and Width of the Z^0-particle from Multi-hadronic Final States Produced in e^+e^- Annihilations." *Phys. Lett.*, **B 231**, 539 (1989).
13.7 SLD, "Direct Measurement of Leptonic Coupling Asymmetries with Polarized Z Bosons." *Phys. Rev. Lett.*, **79**, 804 (1997).

Downloaded from https://www.cambridge.org/core. UNIVERSIDAD AUTONOMA METROPOLITANA, on 10 Nov 2026 at 11:33:25, subject to the Cambridge Core terms of use, available at https://www.cambridge.org/core/terms. https://doi.org/10.1017/9780511609923.015

Volume 231, number 4 PHYSICS LETTERS B 16 November 1989

DETERMINATION OF THE NUMBER OF LIGHT NEUTRINO SPECIES

ALEPH Collaboration

D. DECAMP, B. DESCHIZEAUX, J.-P. LEES, M.-N. MINARD
Laboratoire de Physique des Particules (LAPP), F-74019 Annecy-le-Vieux Cedex, France

J.M. CRESPO, M. DELFINO, E. FERNANDEZ [1], M. MARTINEZ, R. MIQUEL, M.L. MIR, S. ORTEU, A. PACHECO, J.A. PERLAS, E. TUBAU
Laboratorio de Fisica de Altas Energias, Universidad Autonoma de Barcelona, E-08193 Bellaterra (Barcelona), Spain [2]

M.G. CATANESI, M. DE PALMA, A. FARILLA, G. IASELLI, G. MAGGI, A. MASTROGIACOMO, S. NATALI, S. NUZZO, A. RANIERI, G. RASO, F. ROMANO, F. RUGGIERI, G. SELVAGGI, L. SILVESTRIS, P. TEMPESTA, G. ZITO
INFN, Sezione di Bari e Dipartimento di Fisica dell' Università, I-70126 Bari, Italy

Y. CHEN, D. HUANG, J. LIN, T. RUAN, T. WANG, W. WU, Y. XIE, D. XU, R. XU, J. ZHANG, W. ZHAO
Institute of High-Energy Physics, Academia Sinica, Beijing, P.R. China

H. ALBRECHT [3], F. BIRD, E. BLUCHER, T. CHARITY, H. DREVERMANN, Ll. GARRIDO, C. GRAB, R. HAGELBERG, S. HAYWOOD, B. JOST, M. KASEMANN, G. KELLNER, J. KNOBLOCH, A. LACOURT, I. LEHRAUS, T. LOHSE, D. LÜKE [3], A. MARCHIORO, P. MATO, J. MAY, V. MERTENS, A. MINTEN, A. MIOTTO, P. PALAZZI, M. PEPE-ALTARELLI, F. RANJARD, J. RICHSTEIN [4], A. ROTH, J. ROTHBERG [5], H. ROTSCHEIDT, W. VON RÜDEN, D. SCHLATTER, R. ST.DENIS, M. TAKASHIMA, M. TALBY, H. TAUREG, W. TEJESSY, H. WACHSMUTH, S. WHEELER, W. WIEDENMANN, W. WITZELING, J. WOTSCHACK
European Organization for Nuclear Research (CERN), CH-1211 Geneva 23, Switzerland

Z. AJALTOUNI, M. BARDADIN-OTWINOWSKA, A. FALVARD, P. GAY, P. HENRARD, J. JOUSSET, B. MICHEL, J-C. MONTRET, D. PALLIN, P. PERRET, J. PRAT, J. PRORIOL, F. PRULHIÈRE
Laboratoire de Physique Corpusculaire, Université Blaise Pascal, Clermont-Ferrand, F-63177 Aubière, France

H. BERTELSEN, F. HANSEN, J.R. HANSEN, J.D. HANSEN, P.H. HANSEN, A. LINDAHL, B. MADSEN, R. MØLLERUD, B.S. NILSSON, G. PETERSEN
Niels Bohr Institute, DK-2100 Copenhagen, Denmark [6]

E. SIMOPOULOU, A. VAYAKI
Nuclear Research Center Demokritos (NRCD), Athens, Greece

J. BADIER, D. BERNARD, A. BLONDEL, G. BONNEAUD, J. BOUROTTE, F. BRAEMS, J.C. BRIENT, M.A. CIOCCI, G. FOUQUE, R. GUIRLET, P. MINÉ, A. ROUGÉ, M. RUMPF, H. VIDEAU, I. VIDEAU [1], D. ZWIERSKI
Laboratoire de Physique Nucléaire Hautes Energies, École Polytechnique, F-91128 Palaiseau Cedex, France

0370-2693/89/$ 03.50 © Elsevier Science Publishers B.V.
(North-Holland Physics Publishing Division)

Downloaded from https://www.cambridge.org/core. UNIVERSIDAD AUTONOMA METROPOLITANA, on 10 Nov 2026 at 11:33:25, subject to the Cambridge Core terms of use, available at https://www.cambridge.org/core/terms. https://doi.org/10.1017/9780511609923.015

Volume 231, number 4 PHYSICS LETTERS B 16 November 1989

D.J. CANDLIN
Department of Physics, University of Edinburgh, Edinburgh EH9 3JZ, UK [7]

A. CONTI, G. PARRINI
Dipartimento di Fisica, Università di Firenze, I-50125 Florence, Italy

M. CORDEN, C. GEORGIOPOULOS, J.H. GOLDMAN, M. IKEDA, D. LEVINTHAL [8], J. LANNUTTI, M. MERMIKIDES, L. SAWYER
High-Energy Particle Physics Laboratory, Florida State University, Tallahassee, FL 32306, USA [9,10,11]

A. ANTONELLI, R. BALDINI, G. BENCIVENNI, G. BOLOGNA, F. BOSSI, P. CAMPANA, G. CAPON, V. CHIARELLA, G. DE NINNO, B. D'ETTORRE-PIAZZOLI, G. FELICI, P. LAURELLI, G. MANNOCCHI, F. MURTAS, G.P. MURTAS, G. NICOLETTI, P. PICCHI, P. ZOGRAFOU
Laboratori Nazionali dell' INFN (LNF-INFN), I-00044 Frascati, Italy

B. ALTOON, O. BOYLE, A.J. FLAVELL, A.W. HALLEY, I. TEN HAVE, J.A. HEARNS, I.S. HUGHES, J.G. LYNCH, D.J. MARTIN, R. O'NEILL, C. RAINE, J.M. SCARR, K. SMITH [1], A.S. THOMPSON
Department of Natural Philosophy, University of Glasgow, Glasgow G12 8QQ, UK [7]

B. BRANDL, O. BRAUN, R. GEIGES, C. GEWENIGER [1], P. HANKE, V. HEPP, E.E. KLUGE, Y. MAUMARY, M. PANTER, A. PUTZER, B. RENSCH, A. STAHL, K. TITTEL, M. WUNSCH
Institut für Hochenergiephysik, Universität Heidelberg, D-6900 Heidelberg, FRG [12]

G.J. BARBER, A.T. BELK, R. BEUSELINCK, D.M. BINNIE, W. CAMERON [1], M. CATTANEO, P.J. DORNAN, S. DUGEAY, R.W. FORTY, D.N. GENTRY, J.F. HASSARD, D.G. MILLER, D.R. PRICE, J.K. SEDGBEER, I.R. TOMALIN, G. TAYLOR
Department of Physics, Imperial College, London SW7 2BZ, UK [7]

P. GIRTLER, D. KUHN, G. RUDOLPH
Institut für Experimentalphysik, Universität Innsbruck, A-6020 Innsbruck, Austria

T.J. BRODBECK, C. BOWDERY [1], A.J. FINCH, F. FOSTER, G. HUGHES, N.R. KEEMER, M. NUTTALL, B.S. ROWLINGSON, T. SLOAN, S.W. SNOW
Department of Physics, University of Lancaster, Lancaster LA1 4YB, UK [7]

T. BARCZEWSKI, L.A.T. BAUERDICK, K. KLEINKNECHT, D. POLLMANN [13], B. RENK, S. ROEHN, H.-G. SANDER, M. SCHMELLING, F. STEEG
Institut für Physik, Universität Mainz, D-6500 Mainz, FRG [12]

J.-P. ALBANESE, J.-J. AUBERT, C. BENCHOUK, A. BONISSENT, F. ETIENNE, R. NACASCH, P. PAYRE, B. PIETRZYK [1], Z. QIAN
Centre de Physique des Particules, Faculté des Sciences de Luminy, F-13288 Marseille, France

W. BLUM, P. CATTANEO, M. COMIN, B. DEHNING, G. COWAN, H. DIETL, M. FERNANDEZ-BOSMAN, D. HAUFF, A. JAHN, E. LANGE, G. LÜTJENS, G. LUTZ, W. MÄNNER, H.-G. MOSER, Y. PAN, R. RICHTER, A. SCHWARZ, R. SETTLES, U. STIEGLER, U. STIERLIN, G. STIMPFL [14], J. THOMAS, G. WALTERMANN
Max-Planck-Institut für Physik und Astrophysik, Werner-Heisenberg-Institut für Physik, D-8000 Munich, FRG [12]

Downloaded from https://www.cambridge.org/core. UNIVERSIDAD AUTONOMA METROPOLITANA, on 10 Nov 2026 at 11:33:25, subject to the Cambridge Core terms of use, available at https://www.cambridge.org/core/terms. https://doi.org/10.1017/9780511609923.015

Volume 231, number 4 PHYSICS LETTERS B 16 November 1989

J. BOUCROT, O. CALLOT, A. CORDIER, M. DAVIER, G. DE BOUARD, G. GANIS, J.-F. GRIVAZ, Ph. HEUSSE, P. JANOT, V. JOURNÉ, D.W. KIM, J. LEFRANÇOIS, D. LLOYD-OWEN, A.-M. LUTZ, P. MAROTTE, J.-J. VEILLET
Laboratoire de l'Accélérateur Linéaire, Université de Paris-Sud, F-91405 Orsay Cedex, France

S.R. AMENDOLIA, G. BAGLIESI, G. BATIGNANI, L. BOSISIO, U. BOTTIGLI, C. BRADASCHIA, I. FERRANTE, F. FIDECARO, L. FOÀ [1], E. FOCARDI, F. FORTI, A. GIASSI, M.A. GIORGI, F. LIGABUE, A. LUSIANI, E.B. MANNELLI, P.S. MARROCCHESI, A. MESSINEO, F. PALLA, G. SANGUINETTI, S. SCAPELLATO, J. STEINBERGER, R. TENCHINI, G. TONELLI, G. TRIGGIANI
Dipartimento di Fisica dell' Università, INFN Sezione di Pisa, e Scuola Normale Superiore, I-56010 Pisa, Italy

J.M. CARTER, M.G. GREEN, A.K. McKEMEY, P.V. MARCH, T. MEDCALF, M.R. SAICH, J. STRONG [1], R.M. THOMAS, T. WILDISH
Department of Physics, Royal Holloway & Bedford New College, University of London, Surrey TW20 0EX, UK [7]

D.R. BOTTERILL, R.W. CLIFFT, T.R. EDGECOCK, M. EDWARDS, S.M. FISHER, D.L. HILL, T.J. JONES, G. McPHERSON, M. MORRISSEY, P.R. NORTON, D.P. SALMON, G.J. TAPPERN, J.C. THOMPSON, J. HARVEY
High-Energy Physics Division, Rutherford Appleton Laboratory, Chilton, Didcot, Oxon OX11 0QX, UK [7]

B. BLOCH-DEVAUX, P. COLAS, C. KLOPFENSTEIN, E. LANÇON, E. LOCCI, S. LOUCATOS, L. MIRABITO, E. MONNIER, P. PEREZ, F. PERRIER, B. PIGNARD, J. RANDER, J.-F. RENARDY, A. ROUSSARIE, J.-P. SCHULLER, R. TURLAY
Département de Physique des Particules Elémentaires, CEN-Saclay, F-91191 Gif-sur-Yvette Cedex, France

J.G. ASHMAN, C.N. BOOTH, F. COMBLEY, M. DINSDALE, J. MARTIN, D. PARKER, L.F. THOMPSON
Department of Physics, University of Sheffield, Sheffield S3 7RH, UK [7]

S. BRANDT, H. BURKHARDT, C. GRUPEN, H. MEINHARD, E. NEUGEBAUER, U. SCHÄFER, H. SEYWERD, K. STUPPERICH
Fachbereich Physik, Universität Siegen, D-5900 Siegen, FRG [12]

B. GOBBO, F. LIELLO, E. MILOTTI, F. RAGUSA [15], L. ROLANDI [1]
Dipartimento di Fisica, Università di Trieste e INFN Sezione di Trieste, I-34127 Trieste, Italy

L. BELLANTONI, J.F. BOUDREAU, D. CINABRO, J.S. CONWAY, D.F. COWEN, Z. FENG, J.L. HARTON, J. HILGART, R.C. JARED [16], R.P. JOHNSON, B.W. LECLAIRE, Y.B. PAN, T. PARKER, J.R. PATER, Y. SAADI, V. SHARMA, J.A. WEAR, F.V. WEBER, SAU LAN WU, S.T. XUE and G. ZOBERNIG
Department of Physics, University of Wisconsin, Madison, WI 53706, USA [17]

Received 12 October 1989

The cross-section for $e^+e^- \to$ hadrons in the vicinity of the Z boson peak has been measured with the ALEPH detector at the CERN Large Electron Positron collider, LEP. Measurements of the Z mass, $M_Z = (91.174 \pm 0.070)$ GeV, the Z width $\Gamma_Z = (2.68 \pm 0.15)$ GeV, and of the peak hadronic cross-section, $\sigma_{had}^{peak} = (29.3 \pm 1.2)$ nb, are presented. Within the constraints of the standard electroweak model, the number of light neutrino species is found to be $N_\nu = 3.27 \pm 0.30$. This result rules out the possibility of a fourth type of light neutrino at 98% CL.

Downloaded from https://www.cambridge.org/core. UNIVERSIDAD AUTONOMA METROPOLITANA, on 10 Nov 2026 at 11:33:25, subject to the Cambridge Core terms of use, available at https://www.cambridge.org/core/terms. https://doi.org/10.1017/9780511609923.015

Volume 231, number 4 PHYSICS LETTERS B 16 November 1989

1. Introduction

The Z boson was discovered in 1983 at the $p\bar{p}$ collider at CERN [1,2]. Detailed studies of its properties can now be performed in e^+e^- collisions at LEP. In the standard electroweak model [3], the Z boson is expected to decay with comparable probability into all species of fermions that are kinematically allowed. The decay rate of the Z into light, neutral, penetrating particles such as neutrinos, that would otherwise escape detection, can be measured through an increase in the total width Γ_Z. Detection of additional neutrino species would put in evidence additional fermion families, even if the masses of their charged partners are inaccessible at presently available energies. One additional species of neutrino would result in an increase of 6.6% in Γ_Z. Furthermore the peak cross-section to any detectable final state f is very sensitive to this change and would decrease by 13% for one more neutrino species. This cross-section can be expressed in terms of Γ_Z and of the partial widths, Γ_{ee}, Γ_ν, Γ_f, of the Z into e^+e^-, neutrinos, and the final state f as

$$\sigma_f^{\text{peak}} = \frac{12\pi}{M_Z^2}\frac{\Gamma_{ee}\Gamma_f}{\Gamma_Z^2}(1-\delta_{\text{rad}}) \equiv \sigma_f^0(1-\delta_{\text{rad}}) , \qquad (1)$$

with

$$\Gamma_Z = N_\nu\Gamma_\nu + 3\Gamma_{ee} + \Gamma_{\text{had}} , \qquad (2)$$

where N_ν is the number of light neutrino species. In the particular case where f comprised mostly hadronic final states, uncertainties in the overall scale of partial widths, such as those related to the lack of knowledge of the top quark mass and more generally to electroweak radiative effects, as well as uncertainties in the ratio of hadronic to leptonic partial widths, largely cancel in this formula. The QED initial state radiative correction, δ_{rad}, is quite large, but has been calculated to an accuracy believed to be better than 0.5% by several authors [4].

Cross-sections are measured by taking the ratio of the number of selected Z decays, hereafter referred to as hadronic events, to the number of small angle e^+e^- events from the well calculable Bhabha scattering process, hereafter referred to as luminosity events.

2. Description of the ALEPH detector

The data presented here have been collected with the ALEPH detector during the first three weeks of running at LEP, from 20 September to 9 October 1989. Guided by earlier measurements of the Z mass by the CDF [5] and MarkII [6] Collaborations, data were collected mainly at the Z peak and in the near vicinity of it. Integrated luminosities of 64 nb^{-1} at the peak and 88 nb^{-1} on the sides of the peak were recorded.

A detailed description of the ALEPH detector is in preparation [7]. The principal components relevant for this measurement are:

- The Inner Tracking Chamber, ITC, and 8-layer cylindrical drift chamber with sense wires parallel to the beam axis from 13 cm to 29 cm in radius. Tracks with polar angles from 14° to 166° traverse all 8 layers.
- The large cylindrical Time Projection Chamber, TPC, extending from an inner radius of 31 cm to an outer radius of 180 cm over a length of 4.4 m. Up to 21 space coordinates are recorded for tracks with polar angles from 47° to 133°. Requiring 4 coordinates, tracks are reconstructed down to 15°.
- The Electromagnetic Calorimeter, ECAL, a lead wire-chamber sandwich. The cathode readout is subdivided into a total of 73 728 projective towers. Each

[1] Present address: CERN, CH-1211 Geneva 23, Switzerland.
[2] Supported by CAICYT, Spain.
[3] Permanent address: DESY, D-2000 Hamburg 52, FRG.
[4] Present address: Lecroy, Geneva, Switzerland.
[5] On leave of absence from University of Washington, Seattle, WA 98195, USA.
[6] Supported by the Danish Natural Science Research Council.
[7] Supported by the UK Science and Engineering Research Council.
[8] Supported by SLOAN fellowship, contract BR 2703.
[9] Supported by the US Department of Energy, contract DE-FG05-87ER40319.
[10] Supported by the NSF, contract PHY-8451274.
[11] Supported by the US Department of Energy, contract DE-FC0S-85ER250000.
[12] Supported by the Bundesministerium für Forschung und Technologie.
[13] Permanent address: Institut für Physik, Universität Dortmund, D-4600 Dortmund 50, FRG.
[14] Present address: FSU, Tallahassee, FL 32306, USA.
[15] Present address: INFN, Sezione di Milano, I-20133 Milan, Italy.
[16] Permanent address: LBL, Berkeley, CA 94720, USA.
[17] Supported by the US Department of Energy, contract DE-AC02-76ER00881.

Downloaded from https://www.cambridge.org/core. UNIVERSIDAD AUTONOMA METROPOLITANA, on 10 Nov 2026 at 11:33:25, subject to the Cambridge Core terms of use, available at https://www.cambridge.org/core/terms. https://doi.org/10.1017/9780511609923.015

tower of about $1° \times 1°$ solid angle is read out in three stacks of 10, 23 and 12 layers (respectively 4, 9 and 9 radiation lengths). The signals from the 45 wire planes of each of the 36 modules are also read out. The two endcaps cover polar angles from 11° to 40° and 140° to 169° and the barrel covers polar angles from 40° to 140°.

- The superconducting, solenoidal coil, providing a magnetic field of 1.5 T.
- The Hadron Calorimeter, HCAL, comprised of 23 layers of streamer tubes interleaved in the iron of the magnet return yoke, read out by a total of 4608 projective towers. Signals from each of the tubes are also read out. The modules are rotated in azimuth by ~2° with respect to the electromagnetic calorimeter so that inactive zones do not align in the two calorimeters. The two endcaps and the barrel of the hadron calorimeter cover polar angles down to 6°.
- The Small Angle Tracking chamber, SATR, with 9 planes of drift tubes, covering angles from 40 to 90 mrads, for precise measurement of small angle electron tracks.
- The Luminosity Calorimeter, LCAL, similar in its construction and read-out to ECAL, extending from 50 to 180 mrads, providing energy and position measurement of the showers produced by luminosity events.

Hadronic events were triggered by two independent first level triggers: (i) an ECAL-based trigger, requiring a total energy of 6 GeV deposited in the ECAL barrel or 3 GeV in either of the ECAL endcaps or 1 GeV in both in coincidence; (ii) an ITC–HCAL coincidence, for penetrating charged particles, requiring 6 ITC wire planes and 4 to 8 planes of HCAL tubes in the same azimuthal region.

Luminosity events were also triggered in two ways: (i) a coincidence of 15 GeV deposited in LCAL on one side with 10 GeV deposited on the other side, without requiring azimuthal correlation; (ii) a single arm requirement of 32 GeV deposited in either side of LCAL. In addition, prescaled single arm triggers with 10 and 15 GeV thresholds were recorded to provide an estimate of the beam related background.

All types of events were processed simultaneously through the same trigger system (with the same deadtime), through the same data acquisition and reconstruction programs. In order to ensure that the events were counted during the same life-time, the list of enabled triggers and the status of each of the relevant subdetectors was recorded with each event. Events were accepted only when both ECAL and LCAL were running and when both ECAL and LCAL triggers were enabled. A possible bias could come from the few data acquisition failures that occurred during the run. A careful investigation of all the events before, during, and after each failure revealed a possible but small loss of 0.4% of the hadronic events. This check could be done for the events that were mishandled because their trigger pattern was always recorded and the trigger patterns of hadronic and luminosity events are unique enough to allow an estimate of the losses in each category.

3. Event selection

To provide a check, two independent event selections were used. The first one selected hadronic Z decays only, and was based on TPC tracks. The second one selected decays of the Z into hadrons as well as τ pairs, and was based on calorimetric energy. The event samples overlapped to the extent of 95%. The efficiencies of both methods were very close to unity and systematic uncertainties in these efficiencies were less than 1%. Altogether 3112 events were retained in the track selection and 3320 events in the calorimetric selection.

3.1. Selection with TPC tracks

Hadronic Z decays (a typical event is shown in fig. 1) were selected on the basis of charged tracks only, requiring at least 5 charged tracks. The energy sum of all charged tracks was required to be at least 10% of the centre-of-mass energy. Tracks were required to have a polar angle larger than 18.2°, to be reconstructed from at least 4 TPC coordinates, and to originate from a 2 cm radius 20 cm long cylinder around the nominal beam position. The performance of the TPC was in remarkable agreement with expectations. In order to estimate the acceptance, a complete simulation of the $e^+e^- \rightarrow$hadrons process was performed, including initial state radiation effects and hadronization. The properties that are relevant for acceptance calculation, total charged-particle energy, track multiplicity, sphericity distribution and polar

Downloaded from https://www.cambridge.org/core. UNIVERSIDAD AUTONOMA METROPOLITANA, on 10 Nov 2026 at 11:33:25, subject to the Cambridge Core terms of use, available at https://www.cambridge.org/core/terms. https://doi.org/10.1017/9780511609923.015

Volume 231, number 4 PHYSICS LETTERS B 16 November 1989

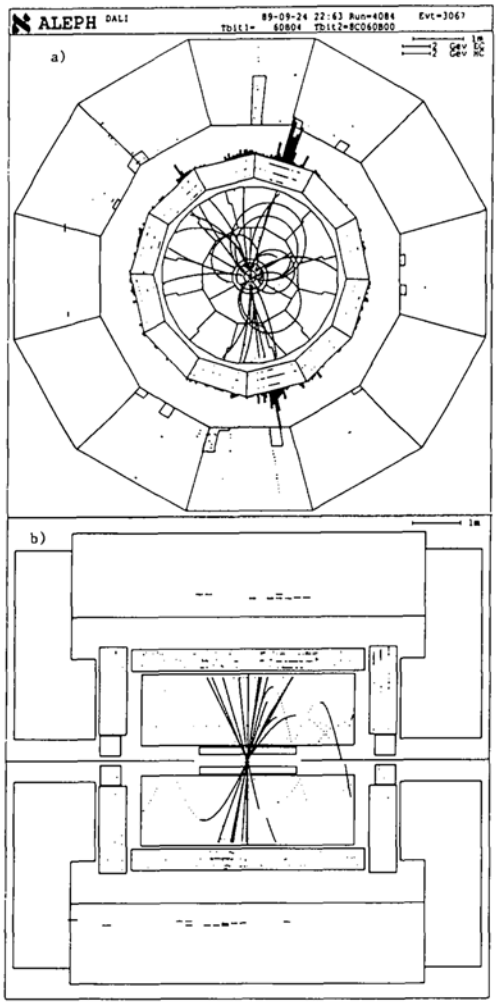


Fig. 1. A hadronic Z decay in the ALEPH detector: (a) x–y view; (b) r–z view.

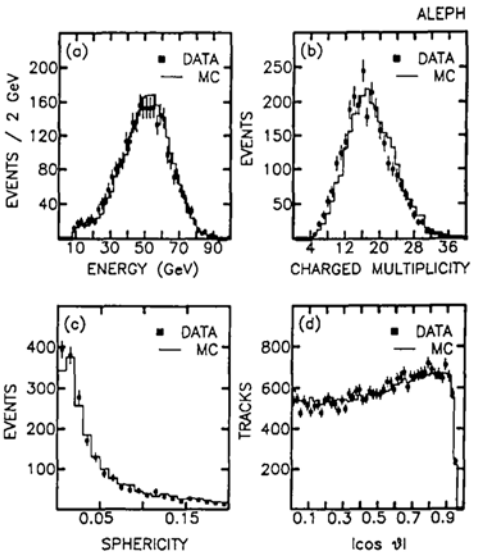


Fig. 2. Properties of charged tracks in hadronic events and comparison with simulations. In each plot, the solid points represent data and the lines represent the simulation normalized to the data: (a) distribution of the charged-track energy sum per event; (b) charged-track multiplicity distribution; (c) sphericity distribution for events where the sphericity axis had a polar angle such that $|\cos\vartheta_{sph}| < 0.8$; and (d) polar angle distribution for charged tracks.

angle distribution, are in good agreement with the simulation, as shown in fig. 2. The efficiency of this selection method is 0.975 ± 0.006, on the peak; the error corresponds to assigning a conservative 20% energy scale uncertainty near the cut. Uncertainties in hadronization models were reduced to a very small level by using the measured sphericity distribution for the acceptance calculation. Due to initial state radiation, this efficiency varies slightly on the side of the Z peak by up to -0.003.

Contamination of the sample of hadronic events by τ pairs from Z decays was estimated to be (5.1 ± 1.5) events, and in fact three events compatible with that hypothesis were found in the sample. Contamination by beam–gas interactions was estimated from the number of events found passing the selection cuts except for the longitudinal vertex position: about one event is expected. Finally the background from $e^+e^- \to e^+e^-$ + hadrons ("two-photon" events) was calculated to be about 15 pb, representing a contamination of 0.5×10^{-3} to the peak cross-section.

Downloaded from https://www.cambridge.org/core. UNIVERSIDAD AUTONOMA METROPOLITANA, on 10 Nov 2026 at 11:33:25, subject to the Cambridge Core terms of use, available at https://www.cambridge.org/core/terms. https://doi.org/10.1017/9780511609923.015

3.2. Selection using the calorimeters

The aim of this method was to select hadronic and τ events. The basic requirement was that the total calorimetric energy be above 20 GeV, as well as either $\geqslant 6$ GeV in the ECAL barrel or at least 1.5 GeV in each ECAL endcap. These requirements reduce both two-photon events and muon-pair events to a negligible level. Large-angle e^+e^- events were rejected on the basis of their characteristic tight energy clusters in the electromagnetic calorimeter. For the few events with no tracks at all, cuts were applied to eliminate cosmic rays: a timing cut and a cut on the minimal number (2) of clusters above 3 GeV in ECAL. On the basis of Monte Carlo simulation as well as the scanning of events the resulting selection efficiency is 0.994 ± 0.005 for hadronic events and 0.60 ± 0.05 for τ events, giving a combined $\sigma_{had} + \sigma_\tau$ efficiency of 0.974 ± 0.006. Contamination by events other than hadronic or τ was estimated to be less than 0.4%.

The two event samples were compared event by event. Differences were well understood given the different characteristics of the two selections.

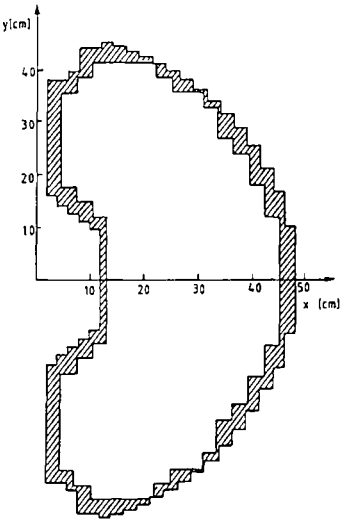


Fig. 3. End view of the Luminosity Calorimeter, showing the tower limits; the shaded area represent the towers excluded from the fiducial area.

3.3. Trigger efficiency

The trigger efficiency was measured by counting events where one or both of the ECAL and ITC–HCAL triggers occurred; it was found to be 100% for the ECAL trigger and 87% for the ITC–HCAL trigger, giving an overall efficiency of 100%.

4. Determination of the luminosity

Luminosity events were selected on the basis of the energy deposited in the LCAL towers. Neighboring towers containing more than 50 MeV were joined into clusters, giving energy and position of the shower. Events were required to have a shower reconstructed on each side of LCAL.

In order to minimize the dependence of the acceptance upon precise knowledge of the beam parameters, an asymmetric selection was performed: on one side (e.g., the e^+ side), showers were required to have more than half of their energy deposited in a fiducial volume (fig. 3) excluding the towers situated at the edge of the detector; the total energy deposit on that side was also required to be larger than 55% of the beam energy; on the other side (e^- side), only a total energy deposition of more than 44% of beam energy was required. The respective roles of the e^+ and e^- sides were interchanged in every other event. Finally, the difference in azimuth, $\Delta\phi$, between the e^+ and the e^- was required to be larger than 170°.

The accepted cross-section was calculated using a first order event generator [8] with a full simulation of the detector. The value obtained for the cross-section for Bhabha scattering into the region within these cuts was found to be $(31.12 \pm 0.45_{exp} \pm 0.31_{th})$ nb, at a centre-of-mass energy of 91.0 GeV and for a Z mass of 91.0 GeV. the first error represents the effect of uncertainties in the simulation, calibration, and positioning of the apparatus; the second one represents the possible error due to neglecting higher order radiative effects, and the uncertainty in the photon vacuum polarization [9]. Properties of the luminosity events are shown in fig. 4, and compared with the simulation. The optimum energy resolution has not yet been obtained, but the acceptance is quite insensitive to this. Other properties are in good agreement with expectations. The displacements of the beam

Downloaded from https://www.cambridge.org/core. UNIVERSIDAD AUTONOMA METROPOLITANA, on 10 Nov 2026 at 11:33:25, subject to the Cambridge Core terms of use, available at https://www.cambridge.org/core/terms. https://doi.org/10.1017/9780511609923.015

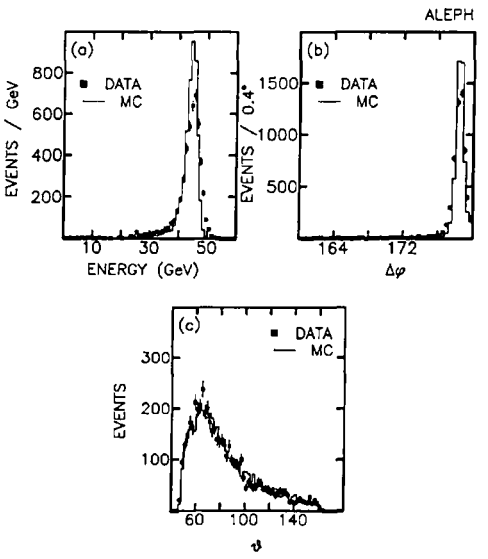


Fig. 4. Properties of luminosity events passing selection criteria and comparison with simulations. In each plot, the solid points represent data and the lines represent the simulation normalized to the data: (a) shower energy distribution for events passing the tight fiducial cut; (b) azimuthal separation $\Delta\phi$ of the two opposite clusters; (c) polar angle distribution.

were measured using luminosity events themselves and corrected for.

The beam-related background contamination was estimated from single arm, prescaled triggers. These triggers were combined into artificial double arm events. The number of such combinations passing the selection cuts was normalized to the number of real coincidences with $\Delta\phi < 90°$. This background subtraction was performed for each run and was of the order of 1% or smaller.

The contamination by physics sources such as $e^+e^- \to \gamma\gamma$ or $e^+e^- \to e^+e^-f\bar{f}$ has been estimated to be less than 2×10^{-3}. The interference of the Z exchange diagram with the purely QED contribution has been taken into account when determining the resonance parameters.

The trigger efficiency was measured for each data taking period by comparing the number of events passing the selection criteria that set the single arm trigger, the coincidence trigger, or both. Inefficiencies in the trigger were traced down to faulty electronic channels. Efficiencies vary with the run, ranging from 0.98 to 1.00 with an average value of 0.997 ± 0.002.

Table 1
Summary of systematic errors in the luminosity measurement.

transverse and longitudinal shower profile	±0.005
energy scale	±0.002
energy resolution and cell-to-cell calibration	±0.007
external alignment and beam parameters	±0.002
internal alignment and inner radius	±0.010
description of material	±0.005
higher order radiative effects	±0.01
total uncertainty:	±0.02

A summary of the luminosity systematic errors is given in table 1. A relatively small normalization error was possible mainly as a result of the excellent spatial resolution of the calorimeter (~ 300 μm for electrons near the tower boundaries), the good background conditions delivered by the machine, the availability of a redundant set of triggers and progress in the theoretical calculations [10]. The relative normalization uncertainty of cross-section measurements at different energies comes mostly from differences in background conditions and trigger efficiency. These uncertainties were taken into account in the statistical error.

5. Determination of the Z resonance parameters

The number of Z events, of luminosity events, together with the cross-sections are given in table 2 for the two event selection methods.

Two different fits were performed to the data. In the first fit, the basic parameters of the Z resonance, its mass M_Z, width Γ_Z, and QED corrected peak cross-section

$$\sigma_f^0 \equiv \frac{12\pi}{M_Z^2} \frac{\Gamma_{ee}\Gamma_f}{\Gamma_Z^2}$$

are extracted with little model dependence. In the second fit, the constraints from the standard model are applied to determine M_Z and N_ν.

The three parameter fit was performed using com-

Downloaded from https://www.cambridge.org/core. UNIVERSIDAD AUTONOMA METROPOLITANA, on 10 Nov 2026 at 11:33:25, subject to the Cambridge Core terms of use, available at https://www.cambridge.org/core/terms. https://doi.org/10.1017/9780511609923.015

Table 2
Event numbers and cross-section as a function of centre-of-mass energy. The overall systematic error of ±2% in the cross-sections is not included.

Energy GeV	Selection from TPC tracks			Selection by calorimeters		
	N_{had}	N_{lumi}	σ_{had} (nb)	$N_{had}+N_\tau$	N_{lumi}	$\sigma_{had}+\sigma_\tau$ (nb)
89.263	120	443	9.00±0.92	134	450	9.89±0.97
90.265	406	715	18.43±1.14	445	736	19.62±1.17
91.020	656	668	31.29±1.72	678	669	32.28±1.76
91.266	1156	1295	28.16±1.14	1243	1309	29.96±1.19
92.260	258	377	21.11±1.72	268	374	22.10±1.78
92.519	125	247	15.52±1.71	142	260	16.75±1.76
93.264	391	883	13.36±0.82	410	889	13.92±0.84

puter programs by Burgers [11] and Borelli et al. [12], folding a Breit–Wigner resonance (with s-dependent width) with the second order exponentiated initial state radiation spectrum. Results from fitting with the two programs were in good agreement with each other. These approximate programs agree adequately with complete electroweak calculations (see D.Y. Bardin et al., in ref. [4] and ref. [13]) for centre-of-mass energies within ±2.5 GeV of the peak. These fits yield the values for the mass and width of the Z boson shown in table 3.

The data points and the result of the fit are shown in fig. 5 for the track selected events.

The error in M_Z does not yet include the uncertainty in the mean e^+e^- collision energy. This error was determined by the LEP division [14] on the basis of measurements of uncertainties in the magnetic field integrals and in the orbit positions to be 5×10^{-4} or 45 MeV. Including this uncertainty, we find

$$M_Z = (91.174 \pm 0.055_{exp} \pm 0.045_{LEP})\ \text{GeV}\,. \qquad (3)$$

The value agrees with the two previous best measurements, refs [5,6], but the uncertainty is smaller by a factor of 2.

M_Z is effectively uncorrelated with the other two parameters. The correlation between Γ_Z and σ^0 for the track selected data sample is shown in fig. 6.

In the standard model, Γ_{ee}, Γ_{had} and Γ_ν are calculable with a small uncertainty of about ±1% due to (i) electroweak radiative effects involving unknown

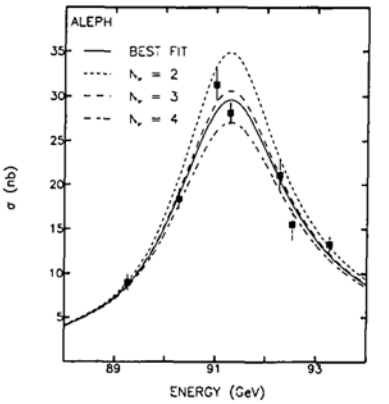


Fig. 5. The cross-section for $e^+e^-\to$hadrons as a function of centre-of-mass energy and result of the three parameter fit.

Table 3

	M_Z (GeV)	Γ_Z (GeV)	σ^0 (nb)	σ^{peak} (nb)
hadronic events	91.178±0.055	2.66±0.16	39.1±1.6	29.3±1.2
hadronic+τ events	91.170±0.054	2.70±0.15	40.9±1.7	30.5±1.3
combined	91.174±0.054	2.68±0.15		

Downloaded from https://www.cambridge.org/core. UNIVERSIDAD AUTONOMA METROPOLITANA, on 10 Nov 2026 at 11:33:25, subject to the Cambridge Core terms of use, available at https://www.cambridge.org/core/terms. https://doi.org/10.1017/9780511609923.015

Volume 231, number 4 PHYSICS LETTERS B 16 November 1989

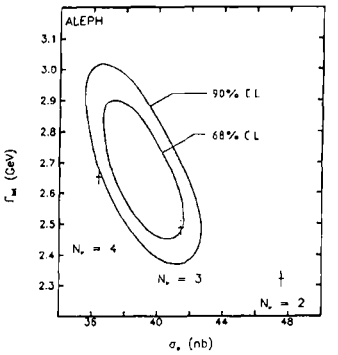


Fig. 6. The total width versus the peak hadronic cross-section, with 68% and 90% CL experimental contours. The standard model prediction for 2, 3 or 4 species of neutrinos is also shown, with its theoretical error.

Table 4
Standard model partial widths of the Z in MeV for the measured value of M_Z; $\alpha_s = 0.12 \pm 0.02$ and $\sin^2\theta_w = 0.230 \pm 0.006$ have been used as input.

Γ_{ee} (MeV)	83.5± 0.5
Γ_ν (MeV)	166.5± 1.0
Γ_{had} (MeV)	1737 ±22

particles, such as the top quark; (ii) the value of the strong coupling constant α_s. The standard model predictions for the partial widths are given in table 4. The standard model predictions for σ^0 and Γ_Z assuming 2, 3, and 4 species of light neutrinos are shown in fig. 6. The value $N_\nu = 3$ is preferred. More precise information on N_ν is contained in the peak cross-section σ^0.

If the partial widths are taken from standard model predictions, a two parameter fit can be performed, leaving M_Z and N_ν as only free parameters. This fit, performed with the programs of refs. [12,15] on the two data samples, leaves the value of M_Z unchanged. The result for N_ν is

$$N_\nu = 3.27 \pm 0.24_{stat} \pm 0.16_{sys} \pm 0.05_{th}\,, \qquad (4)$$

where the errors coming from statistics, experimental systematics and theoretical uncertainty are shown separately. Theoretical uncertainties due to electroweak radiative effects consist mostly in a change of the overall scale of the partial widths, and largely cancel in σ^0. The uncertainty in Γ_{had}, related to the QCD correction, cancels in part in σ^0; the resulting uncertainty $\Delta\sigma^0/\sigma^0 = 0.4\Delta\Gamma_{had}/\Gamma_Z = 0.003$ is much smaller than the effect produced by a single neutrino family, $\Delta\sigma^0/\sigma^0 = -0.13$. Combining these errors in quadrature one finds

$$N_\nu = 3.27 \pm 0.30\,. \qquad (5)$$

The hypothesis $N_\nu = 4$ is ruled out at 98% confidence level. This measurement improves in a decisive way upon previous determinations of the number of neutrino species from the UA1 [16] and UA2 [17] experiments, from PEP [18] and PETRA [19], from cosmological [20] or astrophysical [21] arguments, as well as from a similar determination at the Z peak [22].

The demonstration that there is a third neutrino confirms that the τ neutrino is distinct from the e and μ neutrinos. The absence of a fourth light neutrino indicates that the quark–lepton families are closed with the three which are already known, except for the possibility that higher order families have neutrinos with masses in excess of ~30 GeV.

Acknowledgement

We would like to express our gratitude and admiration to our colleagues of the LEP division for the timely and beautiful operation of the machine. We thank the Technical Coordinator, Pierre Lazeyras, and the technical staff of the ALEPH Collaboration for their excellent work. We would like to dedicate this paper to the memory of those who died during LEP construction: Luigi Barito, Miloud Ferras, Luigi Filippi, Frédéric Mouly, Noël Piccini and François Pierrus. Those of us from non-member countries thank CERN for its hospitality.

References

[1] UA1 Collab., G. Arnison et al., Phys. Lett. B 126 (1983) 398.
[2] UA2 Collab., P. Bagnaia et al., Phys. Lett. B 129 (1983) 130.

Downloaded from https://www.cambridge.org/core. UNIVERSIDAD AUTONOMA METROPOLITANA, on 10 Nov 2026 at 11:33:25, subject to the Cambridge Core terms of use, available at https://www.cambridge.org/core/terms. https://doi.org/10.1017/9780511609923.015

[3] S.L. Glashow, Nucl. Phys. 22 (1961) 579;
S. Weinberg, Phys. Rev. Lett. 19 (1967) 1264;
A. Salam, Elementary particle theory, ed. N. Svartholm (Almquist and Wiksell, Stockholm, 1968) p. 367.
[4] For references see D.Y. Bardin et al., Z-line-shape group, in: Proc. Workshop of Z physics at LEP, CERN report 89-08;
R.N. Cahn, Phys. Rev. D 36 (1987) 2666;
O. Nicrosini and L. Trentadue, Phys. Lett. B 196 (1987) 551;
F.A. Berends, G. Burgers, W. Hollik and W.L. van Neerven, Phys. Lett. B 203 (1988) 177;
G. Burgers, in: Polarization at LEP, preprint CERN 88-06 (1988);
D.C. Kennedy et al., Nucl. Phys. B 321 (1989) 83.
[5] F. Abe et al., Phys. Rev. Lett. 63 (1989) 720.
[6] G.S. Abrams et al., Phys. Rev. Lett. 63 (1989) 724.
[7] ALEPH – a detector for electron–positron annihilation at LEP, Nucl. Instrum. Methods, to be published.
[8] F.A. Berends and R. Kleiss, Nucl. Phys. B 228 (1983) 737;
M. Böhm, A. Denner and W. Hollik, Nucl. Phys. B 304 (1988) 687;
F.A. Berends, R. Kleiss and W. Hollik, Nucl. Phys. B 304 (1988) 712.
[9] H. Burkhardt, F. Jegerlehner, G. Penso and C. Verzegnassi, Z. Phys. C 43 (1989) 497.
[10] D.Y. Bardin et al., Monte Carlo working group, Proc. Workshop of Z physics at LEP, CERN report 89-08.
[11] Computer program ZAPP, courtesy of G. Burgers.
[12] A. Borelli, M. Consoli, L. Maiani and R. Sisto, preprint CERN-TH-5441 (1989).
[13] Computer program ZHADRO, courtesy of G. Burgers.
[14] S. Myers, private communication; and LEP note, to appear.
[15] Computer program ZAPPH, courtesy of G. Burgers.
[16] UA1 Collab., C. Albajar et al., Phys. Lett. B 185 (1987) 241; B 198 (1987) 271.
[17] UA2 Collab., R. Ansari et al., Phys. Lett. B 186 (1987) 440.
[18] MAC Collab., W.T. Ford et al., Phys. Rev. D 19 (1986) 3472.
ASP Collab., C. Hearty et al., Phys. Rev. Lett. 58 (1987) 1711.
[19] CELLO Collab., H.J. Behrend et al., Phys. Lett. B 215 (1988) 186.
[20] G. Steigman, K.A. Olive, D.N. Schramm and M.S. Turner, Phys. Lett. B 176 (1986) 33;
J. Ellis, K. Enqvist, D.V. Nanopoulos and S. Sarkar, Phys. Lett. B 167 (1986) 457.
[21] J. Ellis and K.A. Olive, Phys. Lett. B 193 (1987) 525;
R. Schaeffer, Y. Declais and S. Jullian, Nature 330 (1987) 142;
L.M. Krauss, Nature 329 (1987) 689.
[22] MarkII Collab., J.M. Dorfan, Intern. Europhysics Conf. on High energy physics (Madrid, Spain, September 1989).

Downloaded from https://www.cambridge.org/core. UNIVERSIDAD AUTONOMA METROPOLITANA, on 10 Nov 2026 at 11:33:25, subject to the Cambridge Core terms of use, available at https://www.cambridge.org/core/terms. https://doi.org/10.1017/9780511609923.015